● RESEARCH ARTICLE

Neural stem cell transplantation inhibits glial cell proliferation and P2X receptor-mediated neuropathic pain in spinal cord injury rats
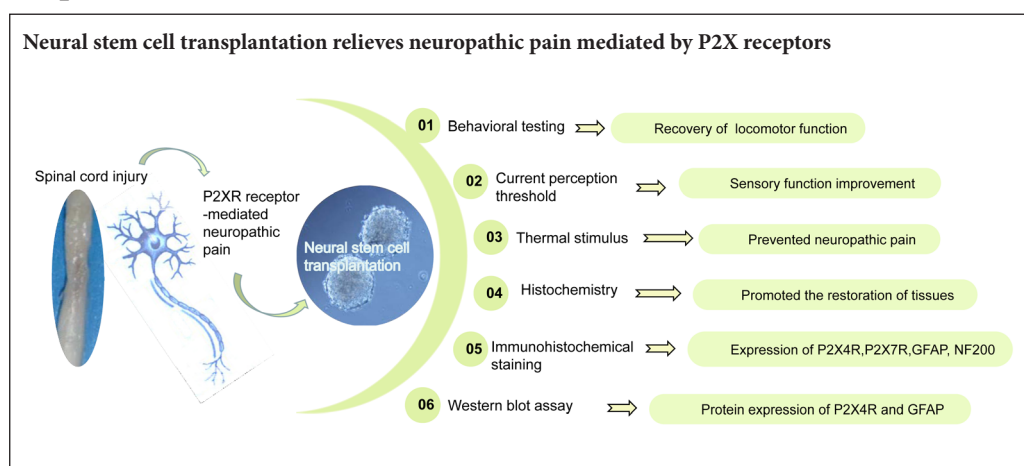
Xiao-Jing Du[1], Yue-Xia Chen[1], Zun-Cheng Zheng[1, *], Nan Wang[2], Xiao-Yu Wang[1], Fan-E Kong[2]

1 Department of Rehabilitation Medicine, the Central Hospital of Taian, Taian, Shandong Province, China
2 Graduate School, Taishan Medical University, Taian, Shandong Province, China

Graphical Abstract

Neural stem cell transplantation relieves neuropathic pain mediated by P2X receptors

Correspondence to:
Zun-Cheng Zheng, MS,
zxyyzhengzuncheng@126.com.

orcid:
0000-0002-2998-1266
(Zun-Cheng Zheng)

Abstract

P2X4 and P2X7 receptors play an important role in neuropathic pain after spinal cord injury. Regulation of P2X4 and P2X7 receptors can obviously reduce pain hypersensitivity after injury. To investigate the role of neural stem cell transplantation on P2X receptor-mediated neuropathic pain and explore related mechanisms, a rat model of spinal cord injury was prepared using the free-falling heavy body method with spinal cord segment 10 as the center. Neural stem cells were injected into the injured spinal cord segment using a micro-syringe. Expression levels of P2X4 and P2X7 receptors, neurofilament protein, and glial fibrillary acidic protein were determined by immunohistochemistry and western blot assay. In addition, sensory function was quantitatively assessed by current perception threshold. The Basso-Beattie-Bresnahan locomotor rating scale was used to assess neuropathological pain. The results showed that 4 weeks after neural stem cell transplantation, expression of neurofilament protein in the injured segment was markedly increased, while expression of glial fibrillary acidic protein and P2X4 and P2X7 receptors was decreased. At this time point, motor and sensory functions of rats were obviously improved, and neuropathic pain was alleviated. These findings demonstrated that neural stem cell transplantation reduced overexpression of P2X4 and P2X7 receptors, activated locomotor and sensory function reconstruction, and played an important role in neuropathic pain regulation after spinal cord injury. Therefore, neural stem cell transplantation is one potential option for relieving neuropathic pain mediated by P2X receptors.

Key Words: *nerve regeneration; cell transplantation; sensory nerve function; glial fibrillary acidic protein; neurofilament; P2X4 receptor; P2X7 receptor; microglial cells; perception threshold; hind limb function; glial hyperplasia; neural regeneration*

Chinese Library Classification No. R456; R364

Introduction

Spinal cord injury (SCI), which can result in the partial loss of spinal cord function including movement, sensory deficits, or dysuria, is commonly caused by trauma or disease. In addition, SCI can lead to neuropathic pain, which is characterized by spontaneous pain, hyperalgesia, abnormal pain, and paresthesia (Soler et al., 2017). Neuropathic pain can persist for months without relief, and no effective treat-

ment is available. In part because of its low toxicity and high efficiency, transplantation of neural stem cells (NSCs) has become an effective strategy for functional repair of SCI or neurological damage in recent years (Hosseini et al., 2015; Deng et al., 2018).

Recent studies have shown that cell transplantation can improve neuroregenerative function by replacing damaged cells to exert a neuroprotective effect (Liu et al., 2018; Rug-

giero et al., 2018; Wang et al., 2018). NSCs are capable of self-renewal, and can differentiate into different neural cell types and repair damaged tissues (Muniswami et al., 2017). Indeed, astrocytes, oligodendrocytes, and neurons can be differentiated from NSCs. Thus, NSC transplantation can be used to treat neural injury and neurodegenerative diseases (Zhang et al., 2015). NSCs can secrete a variety of neurotrophic growth factors, which can protect against excitotoxicity to treat damaged spinal tissues (Franchi et al., 2012; Yan et al., 2017). This also improves the microenvironment after SCI, thereby promoting nerve regeneration and improving movement. However, the role of NSCs in sensory function regulation of SCI rats remains to be further investigated. Recently, NSC transplantation was found to downregulate brain-derived neurotrophic factor and to alleviate hyperalgesia after SCI. It also improved the microenvironment after SCI, thereby enhancing nerve regeneration and functional movement (Levi et al., 2018). Furthermore, this process can be used to change microglial cell phenotypes and reduce spinal cord hyperalgesia after SCI (Zhao et al., 2018). P2X4 receptor (P2X4R), which is expressed on activated microglia, plays an important role in neuropathic pain (Yamashita et al., 2016). Antagonizing P2X4R reverses neuropathic pain caused by sciatic nerve injury. However, the relationship between NSC transplantation, neuropathic pain, and P2X receptor (P2XR) still needs further investigation.

Both the peripheral and central nervous systems can cause neuropathic pain when injured or inflamed (Zheng et al., 2016; Deng et al., 2018). Primary sensory terminals, as well as dorsal horn neurons or astrocytes, release adenosine triphosphate after nerve injury. Adenosine triphosphate binds to P2X4 receptors on the surface of microglia to activate them, which in turn elicits morphological changes, increases their number, and alters their gene expression, including that of neurotransmitter receptors. Microglia in the spinal dorsal horn are subsequently activated, thereby causing Ca^{2+} influx and pain hypersensitivity (Cirillo et al., 2015; Malcangio et al., 2017). Pain hypersensitivity may be associated with bioactive factors released by microglia, including cytokines and neurotrophic factors, and increased brain-derived neurotrophic factor expression. Brain-derived neurotrophic factor is involved in central sensitization and leads to neuropathic pain (Chen et al., 2015). After central sensitization, pain signals become adaptive, such that a protective mechanism is inactivated for functional reconstruction. Thus, blocking upregulation of P2X4R expression in microglia is an effective approach for alleviating neuropathic pain (M'Dahoma et al., 2014).

When a nerve is damaged, it releases an excessive amount of adenosine triphosphate that activates high-affinity P2X7 receptors, which are associated with secondary injury (Li et al., 2017). Anatomical spinal cord damage can be reduced and motor recovery can be improved by antagonizing P2X7 receptors (Kuan et al., 2016). Furthermore, spinal damage can be reduced by inhibiting expression of these receptors. Moreover, the P2X7–p38 pathway has significant effects on neuropathic pain and is possibly associated with interac-

tions between neurons and microglia (Miras-Portugal et al., 2016).

NSC transplantation alleviates neuropathic pain by altering microglial phenotypes after SCI. P2X4 and P2X7 receptors play important roles in central neuropathic pain through microglia activation (Zhang et al., 2014; Kameda et al., 2018). Inhibition of P2X4 and P2X7 receptor upregulation after nerve injury alleviates abnormal pain. However, the role of NSC transplantation in regulating P2XR-mediated neuropathic pain remains to be explored. In this study, NSCs were transplanted into SCI rats with neuropathic pain to investigate the analgesic and therapeutic effects mediated by P2XR during neuropathic pain.

Materials and Methods
Animals
Thirty adult male Sprague-Dawley rats weighing 200–250 g were purchased from Jinan Pengyue Experimental Animal Breeding, China [Animal License No. SCXK (Lu) 20140007]. Rats were housed individually with a 12-hour light/dark cycle for 7 days in a dry and ventilated environment at 23–25°C. All rats had free access to food and water. All invasive experimental procedures were performed with anesthesia to minimize pain in animals. This experiment was conducted according to the United States National Institutes of Health (NIH) Guide for the Care and Use of Laboratory Animals. The protocol was approved by the Animal Ethics Committee of Taishan Medical University of China on March 12, 2016 (approval No. 2016058).

Isolation and culture of primary rat NSCs
NSCs were extracted from the hippocampi of newborn rats. After soaking in 75% alcohol, rats were decapitated and both sides of the cerebral hemisphere were exposed. Both sides of the cerebral hemisphere, olfactory bulbs, and cerebellum were stripped. Next, hippocampal tissues were removed. The pia mater was peeled off and hippocampi were separately placed in Dulbecco's Modified Eagle's Medium (DMEM)/F12 media (Gibco, Paisley, Scotland, UK) and then digested in trypsin (Sigma-Aldrich, St. Louis, MO, USA). Trypsinization was stopped by the addition of DMEM. Cells were resuspended, placed in culture flasks, and cultured in fresh complete medium DMEM/F12 (1:1) containing 20 ng/mL basic fibroblast growth factor, 20 ng/mL epidermal growth factor, 2% B27, and 1% N_2 (all from Abcam, Cambridge, UK). Double-antibiotic concentration was 100,000 U/L penicillin (Sigma-Aldrich) and 10,000 U/L streptomycin. After 7 days, NSC cultures were transferred to a new flask. After this step, contaminating cell types were reduced. Finally, NSCs were planted onto two flasks and cultured complete medium, as described above. Cells were incubated in a 37°C incubator and the medium was replaced every 3 days. Mouse anti-nestin (Abcam) was used to identify the purity of NSCs. The results indicated that more than 90% of cells were positive for nestin. The cell suspension was collected and adjusted to a concentration of 1.0×10^5 cells/μL for transplantation.

Induction of SCI

A rat model of SCI was made 7 days after restraint. Rats were intraperitoneally anesthetized with chloral hydrate (10%; 0.3 mL/100 g). In each rat, a 2 cm-long incision was made in the middle of the back, centered on T10. The paraspinal muscles on both sides were peeled and, finally, the T10 spinous processes and lamina were removed (Yezierski et al., 2005; Sumizono, 2018). The spinal cord was exposed. The rat SCI model was made by an ALLEN'S II impactor (MASCIS Impactor, W.M. Keck Center of Rutgers University, Piscataway, NJ, USA) with a dropping weight 10.0 g from 25-cm above the exposed cord (Hwang et al., 2016; Park et al., 2017).

Successful SCI rat models with neuropathic pain needed to satisfy the following two conditions simultaneously (Gonzalez et al., 2016): spinal tissue edema or hemorrhage, spasmodic wobble of the rat tail, bilateral posterior limb tremor, paralysis, and autophagy after anesthesia; and scratching, licking, even self-mutilation, and grooming behavior to the body below the injury level.

Rats that did not meet these two criteria were excluded and supplemented with eligible rats.

Successful SCI rat models with neuropathic pain were randomly divided into vehicle ($n = 10$) and NSC ($n = 10$) groups. Ten normal rats were randomly selected to form a sham group ($n = 10$), whereby the lamina was removed and spinal cord exposed without impacting the spinal cord.

NSC transplantation

NSCs were implanted immediately after surgery. Rats in the NSC group were injected with 2 µL of cell suspension (containing 2×10^5 cells) under stereotactic localization of T10 segments. After slowly injecting NSCs for 5 minutes, the muscle and skin were sutured. The vehicle group was injected with 2 µL DMEM/F12 at the same site using the same method. Rats that underwent surgery were raised separately. Bicillin (60,000 U/kg, intramuscularly) was administered once a week. Manual bladder pressure was performed until urination function was restored because the procedure causes paralysis in the hind limbs and some rats exhibited hematuria and urinary retention.

Assessment of locomotor behavior

The Basso-Beattie-Bresnahan locomotor rating (BBB) scale was applied at 7, 14, 21, and 28 days after surgery to evaluate motor function in the hind limbs (Lindsay et al., 2017; Ruzicka et al., 2017). The BBB rating scale ranges from 0 to 21. A score of 0 means complete posterior paresis, while a score of 21 indicates that the hind legs have completely normal movement and function.

Current perception threshold

The nociceptive threshold of the three groups was evaluated using a Neurometer® (Neurotron, Baltimore, MD, USA) once a week for 4 weeks. Stimulating electrodes were applied to the plantar surfaces of hind paws. In each rat, hair was removed from the back and a patch dispersion electrode was attached to the skin (SDE-49-4; Neurotron Inc.). Rats were kept awake in a Ballman cage (Natsume, Tokyo, Japan) to be suitable for light restraint. Three sine wave pulses (5, 250, and 2000 Hz) were used to stimulate the plantar surface of rats. The intensity of stimulation gradually increased until rats were stimulated to emit a cry, with an increment of 0.05 mA for 5 and 250 Hz, and 0.1 mA for 2000 Hz. Each current perception threshold value (mA) was measured five times and then averaged.

Thermal stimulus

A plantar algesimeter (IITC, Woodland Hills, CA, USA) was used 7, 14, 21, and 28 days after surgery to evaluate heat radiation and assessment of nociceptive sensitivity. Each rat was placed in a plastic box with an elevated glass floor. A 150 W beam of projective light was focused on the plantar surface of the hind paw of each rat. A time meter was connected to an infrared detector pointing to the plantar surface, which was stimulated for up to 30 seconds to prevent skin damage. This test was conducted three times at 5-minute intervals and then averaged. This device was used to measure the withdrawal time of the heated paw.

Tissue processing

Four weeks after injury, rats were anesthetized with chloral hydrate and perfused with 4% paraformaldehyde (Gibco). Spinal cord segments were collected, fixed in 4% paraformaldehyde for 24 hours, and transferred to 20% sucrose for 48 hours. For further histochemistry and immunohistochemical staining, T9–11 spinal cord segments were longitudinally cut into 10-µm thick cryopreserved sections using a cryostat.

Histochemistry

Slices were fixed with 4% paraformaldehyde for 20 minutes, washed with phosphate-buffered saline (Gibco) and distilled water, stained with hematoxylin for 15 minutes, treated with 0.5–1.0% ethanol hydrochloride for 30 seconds, washed with running water for 3 minutes, washed with distilled water, and stained with 0.1–0.5% eosin for 1–3 minutes. All spinal cord tissues were dehydrated with 70% ethanol for 1–3 minutes and then with 85%, 95%, and 100% ethanol successively for the same duration. Tissues were permeated with xylene, sealed, and observed under a light microscope. Myelination was assessed by Luxol fast blue staining. Spinal cord sections were immersed in 0.1% Luxol fast blue overnight. After rinsing, sections were decolorized with 0.05% lithium carbonate solution for 5 minutes. Tissues were followed up by a graded series of ethanol and 0.5% eosin solution for 1 minute, counterstained with 0.1% cresyl violet, and then washed with 70% and 95% ethanol for 3–5 minutes. Finally, slides were made transparent with xylene and fixed with neutral balsam for optical microscopy (BX46, Olympus, Tokyo, Japan). Three random fields of view from each section were analyzed with imaging software (Image Pro Plus™, MediaCybernetics, Silver Spring, CA, USA). Numbers of positive cells were counted or the percentage of staining intensity was calculated and averaged.

Immunohistochemical staining

Sections were subjected to immunohistochemical staining of glial fibrillary acidic protein (GFAP), neurofilament 200 (NF-200), P2X4R, and P2X7R. Frozen slides were air-dried at room temperature for 10 minutes and washed twice with phosphate-buffered saline for 5 minutes. To eliminate endogenous peroxidase activity, sections were incubated at 24–28°C for 5–10 minutes in 3% H_2O_2. Samples were then washed three times for 2 minutes. Subsequently, antigen retrieval was performed by placing samples in citrate buffer (0.1 M, pH 7.42) at 92–98°C for 10–15 minutes. Sections were cooled for 20 minutes, washed three times with phosphate-buffered saline for 15 minutes, then blocked with 5% goat serum (Gibco) for 1 hour at 37°C. Rabbit anti-GFAP (1:800; Abcam), mouse anti-hypophosphorylated neurofilament H (1:100; Abcam), rabbit anti-P2X7 (1:500; Abcam), and goat anti-P2X4 (1:500; Abcam) antibodies were added and incubated overnight at 4°C. After washing samples with phosphate-buffered saline, biotin-labeled goat anti-rabbit IgG, goat anti-mouse IgG, or rabbit anti-goat IgG (1:1000; all from Abcam) was added and incubated at 37°C for 2 hours. Tissues were then rinsed with phosphate-buffered saline, stained with diaminodibenzidine, washed, and sealed. Sections were observed with an optical microscope, and three random fields were analyzed for each section. Percentages of staining intensity were calculated and averaged.

Western blot assay

All spinal cord tissues (T10 spinous process) obtained at 7, 14, 21, and 28 days were homogenized in lysis buffer (Kangwei Biotechnology, Beijing, China). Equal amounts of proteins were separated by sodium dodecyl sulfate-polyacrylamide gel electrophoresis. Resolved proteins were transferred to a nitrocellulose membrane (Whatman, Dassel, Germany), which was incubated with rabbit anti-GFAP (1:1000), goat anti-P2X4 (1:1000), and anti-β-actin (1:2000; Santa Cruz Biotechnology, Dallas, TX, USA) antibodies overnight at 4°C. Subsequently, membranes were rewarmed, washed, and horseradish peroxidase was added to label the secondary antibody. The β-actin antibody was used as a loading control for all experiments. Immunoreactive bands were visualized with an enhanced chemiluminescence reagent (Beyotime, Beijing, China). Grayscale values of bands were quantified with ImageJ software (NIH). Relative protein expression levels were calculated according to the ratio between target grayscale values and loading control grayscale values.

Statistical analysis

Data are expressed as the mean ± SEM. Experiments were repeated three times. Statistical analysis was performed with the SPSS 14.0 software (SPSS, Chicago, IL, USA) statistical package. BBB scores and histological results were analyzed by one-way analysis of variance followed by Tukey's *post hoc* test. Differences with *P* < 0.05 were considered statistically significant.

Results

Identification of NSCs *in vitro*

When primary NSCs were cultured for 7 days, dozens or even hundreds of cells aggregated into suspended cell spheres for growth. These cell spheres were regular in shape with a dark center and bright edges (**Figure 1A**). A nestin antibody was used to perform immunofluorescence identification of these cells. Neurospheres were immunopositive for nestin, suggesting that they were NSCs (**Figure 1B**).
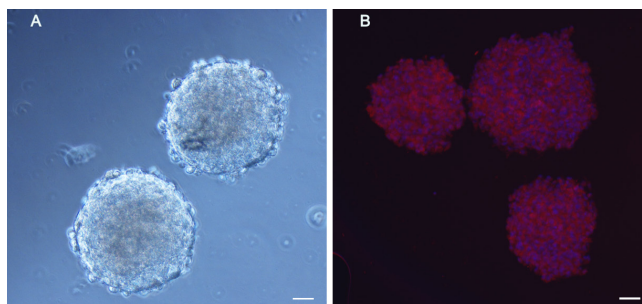

Figure 1 Identification of neural stem cells (NSCs).
NSCs were immunostained with anti-nestin antibody, then labeled with a Cy3-conjugated secondary antibody (red) and Hoechst 33342 (nuclear stain; blue). Characterization of transplanted cells was performed by observing cells under a fluorescence microscope. NSCs extracted from hippocampi of newborn rats were cultured in NSC culture medium. By day 7, the cells had grown in suspension into neurospheres containing hundreds of cells with regular morphology. The peripheries of neurospheres were bright, while the central region had poor transmittance as a result of high cell density (A). Neurospheres were immunopositive for nestin (B). Scale bars: 100 μm.

NSC transplantation improves behavioral recovery after SCI

Motor function of rats with spinal cord injury

The BBB scale was used to evaluate the effect of cell transplantation on motor function. The three groups of rats had normal motor functions before injury, and their scores immediately decreased after injury. NSCs or pure medium was transplanted into the damaged region. The BBB scale was used for weekly evaluations after transplantation. The BBB score of the NSC group gradually increased after transplantation. However, the scores of the rats in the vehicle group remained low. The results showed that NSCs facilitated the recovery of athletic ability (**Figure 2A** and **Table 1**).

Sensory function of rats with spinal cord injury

The sensory function of rats was assessed weekly by current perception threshold. The functional states of three different types of nerve fibers were quantified, each with three current perception threshold stimulation intensities (2 kHz, 250 Hz, and 5 Hz), corresponding to large myelinated (Aβ) fibers, medium myelinated (Aδ) fibers, and unmyelinated (C) fibers. The results showed that the current perception threshold of 5 Hz (**Figure 2B**), 250 Hz (**Figure 2C**), and 2000 Hz (**Figure 2D**) in the NSC group was lower than in the vehicle group, indicating that NSC transplantation considerably ameliorated sensory function (**Table 1**).

Nociceptive sensitivity of rats with spinal cord injury

The nociceptive sensitivity of rats was assessed weekly by thermal stimulus. The results showed that the thermal withdrawal duration of the sham group was maintained within a stable range. However, the thermal withdrawal duration of rats in the NSC group gradually decreased to a normal range. The thermal withdrawal duration of the NSC group was markedly lower than that of the vehicle group (**Figure 2E** and **Table 1**).

Hematoxylin and eosin staining to assess NSC transplantation on histological changes in injured spinal cord

The tissue structure of the sham group was nearly complete, as shown in hematoxylin-eosin-stained sections. Nerve cells were evenly distributed, with normal morphologies and uniform intercellular substances, and nerve fibers were neatly arranged. Four weeks after injury, hematoxylin-eo-sin-stained sections of the vehicle group showed incomplete gray matter and white matter structures, as well as vacuoles and cystic cavities in the injured area, disordered axonal arrangement, and loss of neurons. The NSC group had less severe syringomyelia than the vehicle group (**Figure 3**).

Luxol fast blue staining to assess NSC transplantation on histological changes in injured spinal cord

No abnormalities were observed in spinal cord tissues of the sham group. In contrast, spinal cords in the vehicle group demonstrated obvious signs of compression after SCI, displaying damaged organizational structures. Luxol fast blue-stained sections of the sham group showed neatly arranged myelin sheaths, while blue-stained sections of the vehicle group showed that nerve fibers were sparse, disordered, and exhibited syringomyelia. However, the NSC group had less

Table 1 CPT, BBB score, and thermal withdrawal duration at the fourth week after spinal cord injury

Group	CPT value (mA)			BBB scores	Thermal withdrawal duration (seconds)
	5	250	2000		
Sham	20.50±3.54	35.00±2.83	95.50±0.71	21.00±0.00	10.50±0.78
Vehicle	56.00±1.41	62.50±6.36	136.00±2.83	7.50±0.71	20.80±1.46
NSC	30.50±3.54	39.50±0.71	106.00±1.41	17.50±2.12	11.60±0.82

Data are expressed as the mean ± SEM (one-way analysis of variance followed by Tukey's *post hoc* test). Experiments were performed in triplicate. CPT: Current perception threshold; BBB: Basso-Beattie-Bresnahan locomotor rating scale; NSC: neural stem cells.
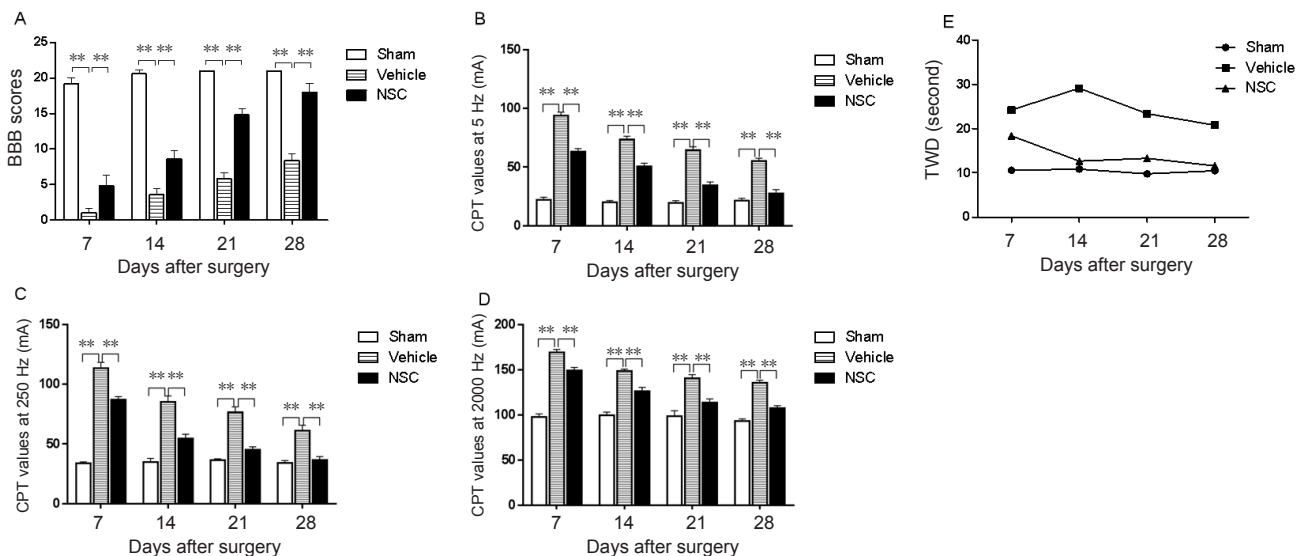

Figure 2 Behavioral recovery after NSC transplantation.
(A) Comparison of BBB scores among the three groups 4 weeks after surgery. After surgery, the recovery of motor function in rats was assessed weekly using the BBB scale for 4 weeks. NSCs or pure medium were transplanted into the spinal cord after injury. The BBB score of the NSC group was significantly improved compared with the vehicle group. ∗∗$P < 0.01$. Data are expressed as the mean ± SEM (one-way analysis of variance followed by Tukey's *post hoc* test). Experiments were performed in triplicate. NSCs considerably improved movement and sensory function. (B–D) CPT scores in sham, vehicle, and NSC groups after surgery at 5 Hz (B), 250 Hz (C), and 2000 Hz (D). Nociceptive threshold of the three groups was evaluated by a Neurometer® once per week for 4 weeks. CPT test had three stimulus intensities, namely 5, 250, and 2000 Hz. The functional status of the three distinct nerve fiber type-large myelinated (Aβ) fibers, medium-size myelinated (Aδ) fibers, and unmyelinated (C) fibers were detected and quantified by measuring the CPT at 5, 250, and 2000 Hz, respectively. The results indicated that NSC transplantation remarkably promoted sensory function, especially for C fibers and Aδ fibers. (E) TWD of the heat-shrinking group in the sham group was maintained within a stable range. TWD: Thermal withdrawal duration; BBB: Basso-Beattie-Bresnahan locomotor rating scale; CPT: current perception threshold; NSC: neural stem cell; SCI: spinal cord injury.

severe syringomyelia than the control group (**Figure 3**). This result indicated that NSCs promoted the restoration of spinal cord tissues.

NSCs inhibits spinal reactive glial hyperplasia and promotes histological regeneration

To observe glial reactive hyperplasia after SCI and explore the role of NSCs in regulating reactive gliosis and histological regeneration, we examined expression of GFAP, which is primarily expressed in astrocytic cells and its concentration is associated with SCI severity. The results showed glial reactive hyperplasia after SCI (**Figure 4**). Astrocytes in the sham group were stained brown-yellow, while synapses were slender and showed spider-like shapes. Moreover, astrocyte proliferation, cell body hypertrophy, and synapse were interconnected in the vehicle group. In the NSC group, the morphology of astrocytes was similar to that of the sham group. As the most expressed protein in neurons, neurofilament protein can reflect not only neuronal morphology after injury, but also their function state. Neurofilament-stained sections showed that neurons in sham and NSC groups were more regular and numerous than in the vehicle group. This result suggested that NSC transplantation after SCI not only reduced excessive proliferation of glial cells, but also provided favorable conditions for functional recovery.

NSC treatment reduces spinal P2XR expression in SCI rats

P2XR was mainly distributed in activated microglial cells. This condition is crucial for the transmission and modulation of information encoding nociceptive neuropathic pain. As such, expression of P2X4R and P2X7R in spinal cord sections was analyzed. The sham group showed normal spinal cord tissue, with microglia that were stained brown-yellow with prominent cell bodies and spider-like shapes. The vehicle group had small microglia with narrow cell bodies and slender synapses, similar to the morphology of microglial cells in the NSC group. The results demonstrated upregulated P2X4R and P2X7R expression in the vehicle group, whereas the NSC group showed the opposite effect (**Figure 5**). Moreover, NSC transplantation relieved neuropathic pain after SCI.

Expression of P2X4R and GFAP in injured spinal cord after transplantation

P2X4R and GFAP levels in sham, vehicle, and NSC groups were assessed through western blot assay. As shown in **Figure 6**, P2X4R and GFAP levels exhibited higher increases in the SCI group than in the sham group. Moreover, considerable decreases in P2X4R and GFAP expression levels were observed after NSC treatment. The results showed that NSCs may regulate neuropathic pain and glial reactive hyperplasia after SCI.

Discussion

SCI can lead to serious dysfunction, and some patients have intractable neuropathic pain characterized by spontaneous or abnormal pain, hyperalgesia, and paresthesia (Gruener et al., 2016). Studies have shown that neuropathic pain can alter neuronal plasticity and regulate glial reactive hyperplasia (Nees et al., 2017). Neuropathic pain can persist for months without relief, and no effective treatment is currently available (Li et al., 2018; Shiao et al., 2018). SCI causes increased P2XR expression in the ipsilateral spinal cord. P2XR, which is mainly expressed on microglia, is important for the mechanism of neuropathic pain pathogenesis caused by nerve injury (McGinley et al., 2017; Schug et al., 2017).

In this study, NSCs were transplanted into SCI rats with neuropathic pain, and then movement, sensory function, glial reactive hyperplasia, and P2XR expression were assessed. The results indicated that NSC transplantation can regulate P2XR expression and inhibit neuropathic pain after SCI.

To study the mechanism by which NSC transplantation provides neuropathic pain relief, NSCs were transplanted into SCI animals to inhibit P2XR signaling. After injury, microglia, which act as central nervous system macrophages, immediately switch from a "stationary" to "activated" state, whereby their numbers increase and morphologies change (Yazdani et al., 2012; Song et al., 2015; Wang et al., 2015). Activation of the P2XR receptor triggers Ca^{2+} entry and produces tactile allodynia (Zhao et al., 2015; Curtis et al., 2018; Yuan et al., 2018). Microglial cells expressing P2XR are key cellular intermediates in the pathogenesis of neuronal injury-induced pain hypersensitivity (Selvarajah et al., 2014; Campero et al., 2015). After transplanting NSCs into SCI rats with neuropathic pain, thermal withdrawal duration and P2XR expression were examined. The results demonstrated downregulated P2X4R and P2X7R expression in the NSC group, whereby thermal withdrawal duration was markedly lower than that of the vehicle group. NSC transplantation decreased P2X4R induction and suppressed neuropathic pain after nerve injury; however, the involved regulatory mechanism requires further study.

In the present study, GFAP expression was decreased, but NF-200 expression was significantly increased in the NSC group compared with the vehicle group. The BBB score showed that recovery of hind limb function was enhanced in the NSC group compared with the vehicle group. Astrocytes react quickly when the central nervous system is stimulated or damaged. One sign of this activation is increased expression of GFAP, an astrocyte marker that indirectly reflects their proliferation and hypertrophy (Nakhjavan-Shahraki et al., 2014). SCI leads to reactive gliosis, which facilitates the formation of a mechanical barrier to prevent axonal regeneration, thereby preventing injury repair, but improving neuronal survival to promote spinal cord repair (Liu et al., 2013; Hulme et al., 2017). Hence, establishing how to adjust reactive glia to an appropriate state by colloidal reaction to positively impact damage repair, block the mechanical hindrance of axonal regeneration, and create a microenvironment conducive to SCI repair are directions of future research (Gwak et al., 2017; Hergenroeder et al., 2018). Our results indicate that NSC transplantation can effectively
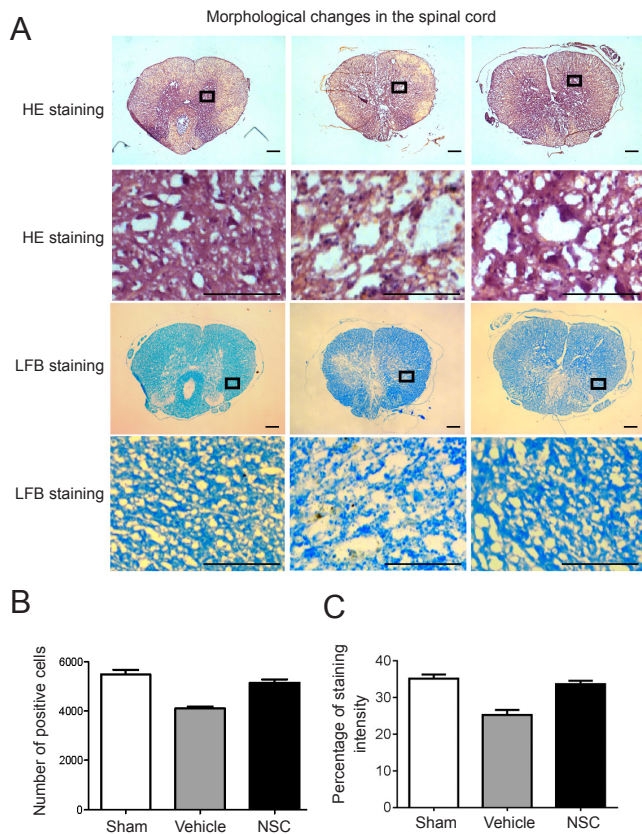
Figure 3 HE and LFB staining of sham, vehicle, and NSC groups at 4 weeks after injury.
(A) Under the light microscope, spinal cords in the vehicle group demonstrated obvious signs of compression following spinal cord injury, such as damaged organizational structures. Three random fields of view from each section were analyzed. Scale bars: 100 μm. (B, C) Number of positive cells or percentage of staining intensity were calculated and averaged. Contents of the pane were enlarged to observe morphological changes. Sham group: Nuclei were regular in shape, deeply stained, and showed neuronal survival. Vehicle group: Nuclei were fragmented and disappeared, the staining was shallow, nerve fibers were unevenly arranged, and fewer neurons survived. NSC group: Nuclei were deeply stained, showed slightly dense cytoplasm, and more neurons survived than in the vehicle group. LFB staining of the sham group revealed neatly arranged myelin sheaths. LFB staining in the vehicle group showed that nerve fibers were sparse, disordered, and formed syringomyelia. LFB-stained sections in the NSC group showed obviously reduced syringomyelia compared with the vehicle group. Data are expressed as the mean ± SEM (one-way analysis of variance followed by Tukey's *post hoc* test). Experiments were performed in triplicate. HE: Hematoxylin-eosin; LFB: Luxol fast blue; NSC: neural stem cell.

Figure 4 Immunofluorescent labeling of GFAP and hypophosphorylated NF-200.
(A) Immunofluorescent labeling of GFAP and NF-200. Expression of GFAP and NF-200 in sham, vehicle, and NSC groups was compared under a light microscope. Contents of the pane were enlarged to observe morphological changes. In the sham group, spinal cord tissue was normal, astrocytes were stained brown-yellow, and synapses were slender and spider-like. In the vehicle group, astrocytes exhibited hypertrophy and synapses were interconnected. In the NSC group, the morphology of astrocytes was similar to that of the sham group. NF-200 staining showed that neurons in sham and NSC groups were more regular and numerous than in the vehicle group. Scale bars: 200 μm. (B) Considerable decreases in GFAP expression levels were observed after NSC treatment. (C) At 4 weeks post transplantation, NF-200 expression in the NSC group was obviously higher than in the vehicle group. Three random fields of view from each section were analyzed. Percentages of staining intensity were calculated and averaged. Data are expressed as the mean ± SEM (one-way analysis of variance followed by Tukey's *post hoc* test). GFAP: Glial fibrillary acidic protein; NF-200: neurofilament 200; NSC: neural stem cells.

reduce glial hyperplasia, weaken factors that impede axon regeneration, and promote the recovery of nerve function.

Electrical stimulation was used to determine the permeability and functional integrity of large myelinated, medium-myelinated, and unmyelinated sensory fibers (Wenzler et al., 2015). Current perception threshold contains three different stimulus frequencies (5, 250, and 2000 Hz). A 5-Hz frequency mainly excited unmyelinated C fibers, which primarily conduct acute pain, chronic pain, temperature sensation, and post-ganglionic sympathetic signals (Hilgenberg-Sydney et al., 2016). By comparison, 250 Hz chiefly excited myelinated Aδ fibers, which rapidly conduct si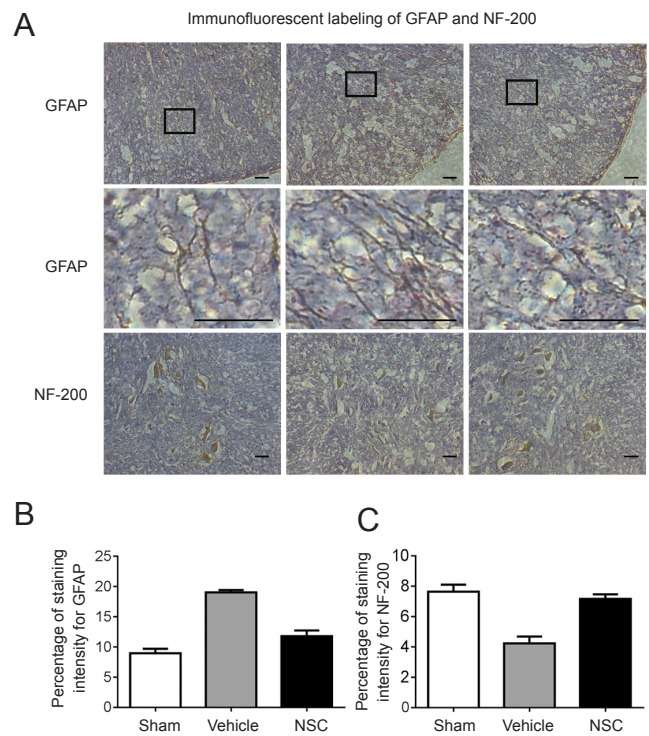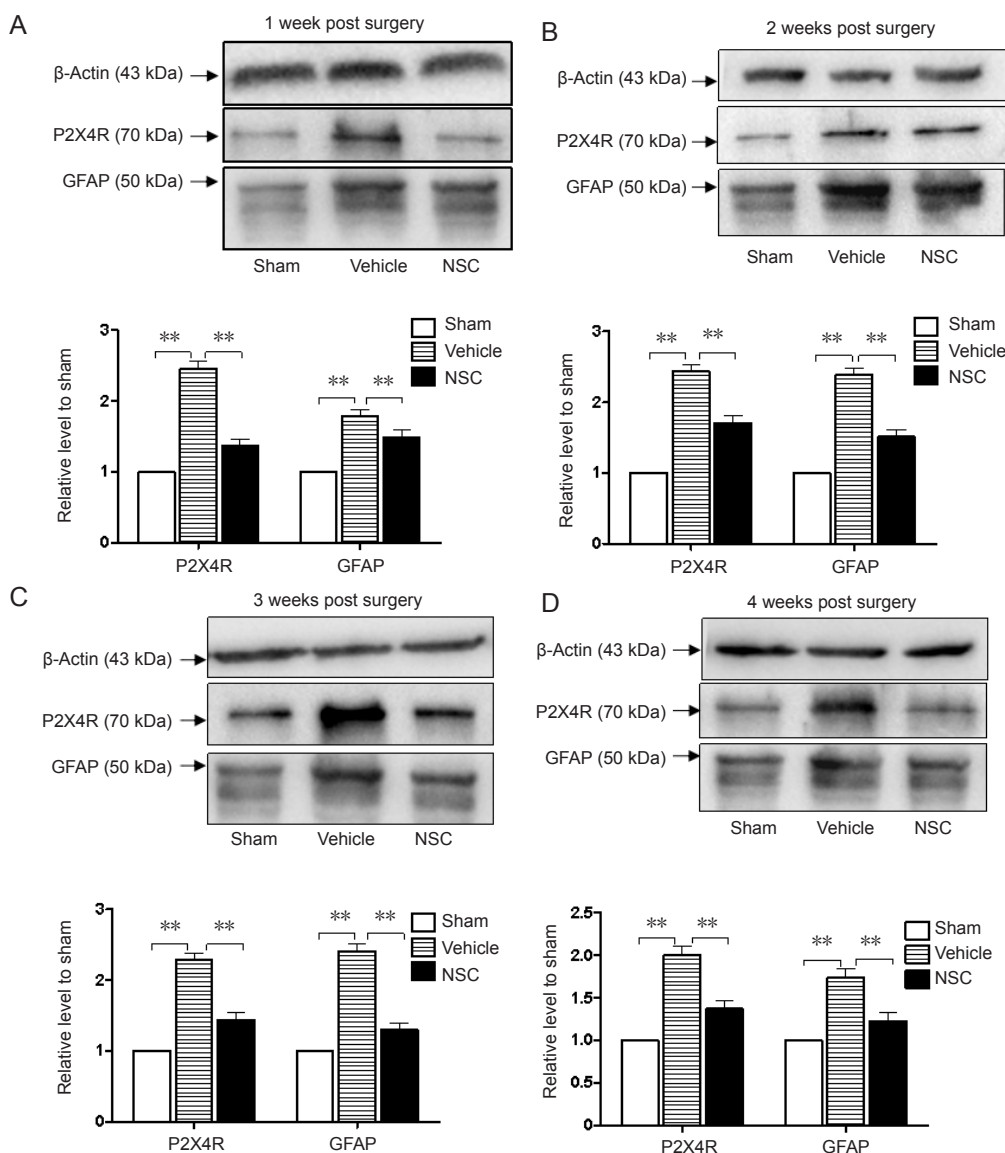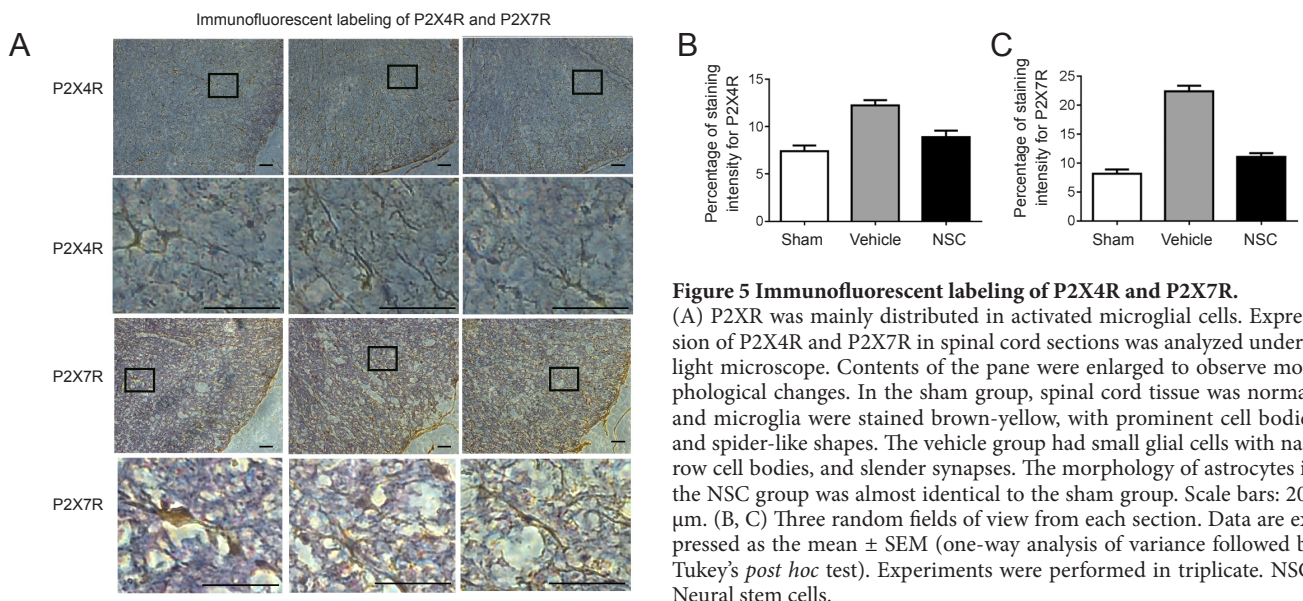gnals from mechanoreceptors, pressure sensation, temperature sensation, and pain. Finally, 2000 Hz mainly excited coarse myelinated Aβ fibers, which conduct skin-contact pressure sensation. After SCI, the conduction bundle was damaged and current perception threshold values were abnormally elevated. These results showed that current perception thresholds of 5, 250, and 2000 Hz were lower in the NSC group compared with the vehicle group, indicating that NSC transplantation considerably ameliorated sensory function. NSC transplantation also remarkably repaired neurological function, possibly by inhibiting GFAP over-expression and glial scar formation to promote nerve fiber regeneration.

In summary, NSC transplantation can suppress the overexpression of P2X4R and GFAP, which inhibits glial scar formation, alleviates central pain, and improves neurological function. Thus, NSC transplantation is a feasible option for regulating central pain after SCI.

Figure 5 Immunofluorescent labeling of P2X4R and P2X7R.
(A) P2XR was mainly distributed in activated microglial cells. Expression of P2X4R and P2X7R in spinal cord sections was analyzed under a light microscope. Contents of the pane were enlarged to observe morphological changes. In the sham group, spinal cord tissue was normal, and microglia were stained brown-yellow, with prominent cell bodies and spider-like shapes. The vehicle group had small glial cells with narrow cell bodies, and slender synapses. The morphology of astrocytes in the NSC group was almost identical to the sham group. Scale bars: 200 μm. (B, C) Three random fields of view from each section. Data are expressed as the mean ± SEM (one-way analysis of variance followed by Tukey's *post hoc* test). Experiments were performed in triplicate. NSC: Neural stem cells.

Figure 6 Expression levels of P2X4R and GFAP proteins in injured spinal cord after transplantation.
Expression levels of GFAP and P2X4 were assessed by western blot assay in the first week (A), second week (B), third week (C) and fourth week (D) after NSC transplantation. Western blot protein levels were normalized to β-actin as a loading control. Relative optical density of protein bands was measured following subtraction of the film background. ****P < 0.01.** Data are expressed as the mean ± SEM (one-way analysis of variance followed by Tukey's *post hoc* test). Experiments were performed in triplicate. P2X4R and GFAP levels exhibited higher increases in the vehicle group compared with the sham group. Considerable decreases in P2X4R and GFAP expression levels were observed after NSC treatment. GFAP: Glial fibrillary acidic protein; NSC: neural stem cells.

References

Campero M, Hughes R, Orellana P, Bevilacqua JA, Guiloff RJ (2018) Spinal cord infarction with ipsilateral segmental neuropathic pain and flaccid paralysis. A functional role for human afferent ventral root small sensory fibres. J Neurol Sci 395:84-87.

Chen XM, Xu J, Song JG, Zheng BJ, Wang XR (2015) Electroacupuncture inhibits excessive interferon-gamma evoked up-regulation of P2X4 receptor in spinal microglia in a CCI rat model for neuropathic pain. Br J Anaesth 114:150-157.

Cirillo G, Colangelo AM, Berbenni M, Ippolito VM, De Luca C, Verdesca F, Savarese L, Alberghina L, Maggio N, Papa M (2015) Purinergic modulation of spinal neuroglial maladaptive plasticity following peripheral nerve injury. Mol Neurobiol 52:1440-1457.

Curtis E, Martin JR, Gabel B, Sidhu N, Rzesiewicz TK, Mandeville R, Van Gorp S, Leerink M, Tadokoro T, Marsala S, Jamieson C, Marsala M, Ciacci JD (2018) A first-in-human, phase I study of neural stem cell transplantation for chronic spinal cord injury. Cell Stem Cell 22:941-950.

Deng J, Zhang Y, Xie Y, Zhang L, Tang P (2018) Cell transplantation for spinal cord injury: tumorigenicity of induced pluripotent stem cell-derived neural stem/progenitor cells. Stem Cells Int 2018:5653787.

Deng Z, Li C, Liu C, Du E, Xu C (2018) Catestatin is involved in neuropathic pain mediated by purinergic receptor P2X4 in the spinal microglia of rats. Brain Res Bull 142:138-146.

Franchi S, Valsecchi AE, Borsani E, Procacci P, Ferrari D, Zalfa C, Sartori P, Rodella LF, Vescovi A, Maione S, Rossi F, Sacerdote P, Colleoni M, Panerai AE (2012) Intravenous neural stem cells abolish nociceptive hypersensitivity and trigger nerve regeneration in experimental neuropathy. Pain 153:850-861.

Gonzalez SL, Coronel MF (2016) Beyond reproduction: the role of progesterone in neuropathic pain after spinal cord injury. Neural Regen Res 11:1238-1240.

Gruener H, Zeilig G, Laufer Y, Blumen N, Defrin R (2016) Differential pain modulation properties in central neuropathic pain after spinal cord injury. Pain 157:1415-1424.

Gwak YS, Hulsebosch CE, Leem JW (2017) Neuronal-glial interactions maintain chronic neuropathic pain after spinal cord injury. Neural Plast 2017:2480689.

Hergenroeder GW, Redell JB, Choi HA, Schmitt L, Donovan W, Francisco GE, Schmitt K, Moore AN, Dash PK (2018) Increased levels of circulating glial fibrillary acidic protein and collapsin response mediator protein-2 autoantibodies in the acute stage of spinal cord injury predict the subsequent development of neuropathic pain. J Neurotrauma 35:2530-2539.

Hilgenberg-Sydney PB, Kowacs PA, Conti PC (2016) Somatosensory evaluation in dysfunctional syndrome patients. J Oral Rehabil 43:89-95.

Hosseini SM, Sani M, Haider KH, Dorvash M, Ziaee SM, Karimi A, Namavar MR (2018) Concomitant use of mesenchymal stem cells and neural stem cells for treatment of spinal cord injury: A combo cell therapy approach. Neurosci Lett 668:138-146.

Hulme CH, Brown SJ, Fuller HR, Riddell J, Osman A, Chowdhury J, Kumar N, Johnson WE, Wright KT (2017) The developing landscape of diagnostic and prognostic biomarkers for spinal cord injury in cerebrospinal fluid and blood. Spinal Cord 55:114-125.

Hwang I, Hahm SC, Choi KA, Park SH, Jeong H, Yea JH, Kim J, Hong S (2016) Intrathecal transplantation of embryonic stem cell-derived spinal gabaergic neural precursor cells attenuates neuropathic pain in a spinal cord injury rat model. Cell Transplant 25:593-607.

Kameda T, Imamura T, Nakashima K (2018) Epigenetic regulation of neural stem cell differentiation towards spinal cord regeneration. Cell Tissue Res 371:189-199.

Kuan YH, Shyu BC (2016) Nociceptive transmission and modulation via P2X receptors in central pain syndrome. Mol Brain 9:58.

Levi AD, Okonkwo DO, Park P, Jenkins AL 3rd, Kurpad SN, Parr AM, Ganju A, Aarabi B, Kim D, Casha S, Fehlings MG, Harrop JS, Anderson KD, Gage A, Hsieh J, Huhn S, Curt A, Guzman R (2018) Emerging safety of intramedullary transplantation of human neural stem cells in chronic cervical and thoracic spinal cord injury. Neurosurgery 82:562-575.

Li CC, Lin HR, Tsai MD, Tsay SL (2018) Neuropathic pain experiences of spinal cord injury patients. J Nurs Res 26:280-287.

Li J, Li X, Jiang X, Yang M, Yang R, Burnstock G, Xiang Z, Yuan H (2017) Microvesicles shed from microglia activated by the P2X7-p38 pathway are involved in neuropathic pain induced by spinal nerve ligation in rats. Purinergic Signal 13:13-26.

Lindsay SL, Toft A, Griffin J, A MME, Barnett SC, Riddell JS (2017) Human olfactory mesenchymal stromal cell transplants promote remyelination and earlier improvement in gait co-ordination after spinal cord injury. Glia 65:639-656.

Liu F, Zou Y, Liu S, Liu J, Wang T (2013) Electro-acupuncture treatment improves neurological function associated with downregulation of PDGF and inhibition of astrogliosis in rats with spinal cord transection. J Mol Neurosci 51:629-635.

Liu XL, Zhao X, Wang C, Gao SJ, Tan YH (2017) Decitabine treatment for acute myeloid leukemia relapse after allogeneic hematopoietic stem cell transplantation. J Biol Regul Homeost Agents 31:171-175.

Malcangio M (2017) Spinal mechanisms of neuropathic pain: is there a P2X4-BDNF controversy? Neurobiol Pain 1:1-5.

McGinley LM, Kashlan ON, Chen KS, Bruno ES, Hayes JM, Backus C, Feldman S, Kashlan BN, Johe K, Feldman EL (2017) Human neural stem cell transplantation into the corpus callosum of Alzheimer's mice. Ann Clin Transl Neurol 4:749-755.

M'Dahoma S, Bourgoin S, Kayser V, Barthelemy S, Chevarin C, Chali F, Orsal D, Hamon M (2014) Spinal cord transection-induced allodynia in rats-behavioral, physiopathological and pharmacological characterization. PLoS One 9:e102027.

Miras-Portugal MT, Gomez-Villafuertes R, Gualix J, Diaz-Hernandez JI, Artalejo AR, Ortega F, Delicado EG, Perez-Sen R (2016) Nucleotides in neuroregeneration and neuroprotection. Neuropharmacology 104:243-254.

Muniswami DM, Kanakasabapathy I, Tharion G (2017) Globose basal cells for spinal cord regeneration. Neural Regen Res 12:1895-1904.

Nakhjavan-Shahraki B, Yousefifard M, Rahimi-Movaghar V, Baikpour M, Nasirinezhad F, Safari S, Yaseri M, Moghadas Jafari A, Ghelichkhani P, Tafakhori A, Hosseini M (2018) Transplantation of olfactory ensheathing cells on functional recovery and neuropathic pain after spinal cord injury; systematic review and meta-analysis. Sci Rep 8:325.

Nees TA, Finnerup NB, Blesch A, Weidner N (2017) Neuropathic pain after spinal cord injury: the impact of sensorimotor activity. Pain 158:371-376.

Park ES, Ahn JM, Jeon SM, Cho HJ, Chung KM, Cho JY, Youn DH (2017) Proteomic analysis of the dorsal spinal cord in the mouse model of spared nerve injury-induced neuropathic pain. J Biomed Res. doi: 10.7555/JBR.31.20160122.

Ruggiero T, Pol R, Camisassa D, Simiele S, Giaccone L, Carossa S (2018) Treatment of symptomatic oral mucositis with sodium hyaluronate and synthetic amino acid precursors of collagen in patients undergoing haematopoietic stem cell transplantation. J Biol Regul Homeost Agents 32:737-743.

Ruzicka J, Machova-Urdzikova L, Gillick J, Amemori T, Romanyuk N, Karova K, Zaviskova K, Dubisova J, Kubinova S, Murali R, Sykova E, Jhanwar-Uniyal M, Jendelova P (2017) A comparative study of three different types of stem cells for treatment of rat spinal cord injury. Cell Transplant 26:585-603.

Schug SA, Parsons B, Almas M, Whalen E (2017) Effect of concomitant pain medications on response to pregabalin in patients with postherpetic neuralgia or spinal cord injury-related neuropathic pain. Pain Physician 20:E53-E63.

Selvarajah S, Hammond ER, Haider AH, Abularrage CJ, Becker D, Dhiman N, Hyder O, Gupta D, Black JH 3rd, Schneider EB (2014) The burden of acute traumatic spinal cord injury among adults in the united states: an update. J Neurotrauma 31:228-238.

Shiao R, Lee-Kubli CA (2018) Neuropathic pain after spinal cord injury: challenges and research perspectives. Neurotherapeutics doi: 10.1007/s13311-018-0633-4.

Soler MD, Morina D, Rodriguez N, Sauri J, Vidal J, Navarro A, Navarro X (2017) Sensory symptom profiles of patients with neuropathic pain after spinal cord injury. Clin J Pain 33:827-834.

Song YY, Peng CG, Ye XB (2015) Combination of edaravone and neural stem cell transplantation repairs injured spinal cord in rats. Genet Mol Res 14:19136-19143.

Sumizono M, Sakakima H, Otsuka S, Terashi T, Nakanishi K, Ueda K, Takada S, Kikuchi K (2018) The effect of exercise frequency on neuropathic pain and pain-related cellular reactions in the spinal cord and midbrain in a rat sciatic nerve injury model. J Pain Res 11:281-291.

Wang D, Zhang J (2015) Effects of hypothermia combined with neural stem cell transplantation on recovery of neurological function in rats with spinal cord injury. Mol Med Rep 11:1759-1767.

Wang YH, Yang ZQ, Zhu SF, Gao Y (2018) Comparative study of methotrexate and human umbilical cord mesenchymal stem cell transplantation in the treatment of rheumatoid arthritis. J Biol Regul Homeost Agents 32:599-605.

Wenzler DL, Burks FN, Cooney M, Peters KM (2015) Proof of concept trial on changes in current perception threshold after sacral neuromodulation. Neuromodulation 18:228-232.

Yamashita T, Yamamoto S, Zhang J, Kometani M, Tomiyama D, Kohno K, Tozaki-Saitoh H, Inoue K, Tsuda M (2016) Duloxetine inhibits microglial P2X4 receptor function and alleviates neuropathic pain after peripheral nerve injury. PLoS One 11:e0165189.

Yan HY, Song LM, Liu Y, Yao G, Zhang RY (2017) Role of sufentanil in neural stem cells transplantation for spinal cord injury. Zhongguo Zuzhi Gongcheng Yanjiu 21:4050-4056.

Yazdani SO, Pedram M, Hafizi M, Kabiri M, Soleimani M, Dehghan MM, Jahanzad I, Gheisari Y, Hashemi SM (2012) A comparison between neurally induced bone marrow derived mesenchymal stem cells and olfactory ensheathing glial cells to repair spinal cord injuries in rat. Tissue Cell 44:205-213.

Yezierski RP (2005) Spinal cord injury: a model of central neuropathic pain. Neurosignals 14:182-193.

Yuan H, Ouyang S, Yang R, Li S, Gong Y, Zou L, Jia T, Zhao S, Wu B, Yi Z, Liu H, Shi L, Li L, Gao Y, Li G, Xu H, Liu S, Zhang C, Liang S (2018) Osthole alleviated diabetic neuropathic pain mediated by the P2X4 receptor in dorsal root ganglia. Brain Res Bull 142:289-296.

Zhang C, Tu F, Zhang JY, Shen L (2014) E-cadherin-transfected neural stem cells transplantation for spinal cord injury in rats. Huazhong Keji Daxue Xuebao (Yixue Yingdewen Ban) 34:554-558.

Zhang J, Liu Z, Chen H, Duan Z, Zhang L, Chen L, Li B (2015) Synergic effects of EPI-NCSCs and OECs on the donor cells migration, the expression of neurotrophic factors, and locomotor recovery of contused spinal cord of rats. J Mol Neurosci 55:760-769.

Zhao Y, Zhang L, Wang M, Yu J, Yang J, Liu A, Yao H, Liu X, Shen Y, Guo B, Wang Y, Wu S (2018) Anxiety specific response and contribution of active hippocampal neural stem cells to chronic pain through wnt/beta-catenin signaling in mice. Front Mol Neurosci 11:296.

Zhao Y, Zuo Y, Wang XL, Huo HJ, Jiang JM, Yan HB, Xiao YL (2015) Effect of neural stem cell transplantation combined with erythropoietin injection on axon regeneration in adult rats with transected spinal cord injury. Genet Mol Res 14:17799-17808.

Zheng Z, Du X, Zhang K, Wang X, Chen Y, Kuang N, Fan T, Sun B (2017) Olfactory ensheathing cell transplantation inhibits P2X4 receptor overexpression in spinal cord injury rats with neuropathic pain. Neurosci Lett 651:171-176.